

Subhalf-Micron Mask Defect Detectability and Printability at 1X Reticle Magnification

Dan Schurz, Warren W. Flack, Gary Newman
Ultratech Stepper, Inc.
San Jose, CA 95134

There have been several studies on the printability of subhalf-micron defects using reduction steppers [1,2]. These studies typically involve 1X reticles with defect sizes greater than 0.3 μm . Because submicron 1X projection systems are being incorporated into numerous fabrication lines, there is a clear need to determine the impact of subhalf-micron defects using these systems. This paper examines defect detection and measurement capability on 1X reticles and the printability of those defects on production submicron 1X steppers. This analysis will enhance the understanding of the relationship between defect size and 1X projection optics and allows for determination of optimal defect specifications.

A test reticle representative of a 64 Mb DRAM metal layer was manufactured with a programmed series of attached and isolated defects ranging from 0.15 to 0.5 μm . Both clear and opaque polarity defects were designed. The defects were identified and measured on two different reticle autoinspection systems. The performance of the two systems was compared to the reticle database to evaluate capture rates and efficiency. Actual reticle defect sizes were measured using low voltage SEM metrology.

Defect printability was determined using a 1X i-line projection stepper with focus and exposure optimized for nominal critical dimensions (CD). The defects that printed on the wafer were measured and compared to the defects measured on the reticle. The effects of varying wafer exposure dose and focus within a 10 percent CD process window on defect printability were also evaluated. The results of the mask inspection comparison and the reticle versus wafer defect maps are compared.

Key Words: subhalf-micron defects, defect printability, submicron 1X steppers, reticle autoinspection systems

1.0 INTRODUCTION

Considerable attention is being given to the printability of reticle defects and their impact on device yields as the semiconductor industry embraces subhalf-micron designs [1, 2, 3]. These

studies typically involve 5X reticles and have shown that defect printability is dependent on defect type, size, location and stepper illumination. In general, these studies have emphasized larger defects because of the 5X reduction optics in the stepper [4]. However, as wafer lithography systems improve their resolution, small reticle defects that were previously insignificant have the potential to cause yield loss and reliability problems. The risk from small defects is heightened by the application of optical proximity correction (OPC) structures such as serifs and unresolved auxiliary patterns on reduction reticles [5]. Submicron 1X reticles and advanced 5X reticles utilizing OPC tend to have similar reticle geometries. These OPC features typically are subhalf-micron on the reticle which presents new issues for reticle manufacturing. For example, Sohn et. al. from Samsung have reported that they expect reticle features of 0.6 μm and OPC features of 0.3 μm on 1 Gb DRAM reticle sets by the year 2000 [6].

Historically, there have been limited data concerning the printability of reticle defects on 1X reticles. Earlier studies found that isolated defects smaller than 0.6 μm did not print on 1.2 μm line and space patterns using an Ultratech 1000 series stepper [7]. Because submicron resolution 1X steppers are currently widely utilized in a variety of fabrication lines, it is important to evaluate the impact of subhalf-micron defects [8]. This paper examines the assumption that clear and opaque defect printability on 1X projection lithography systems is subject to the same variables and behavior as reduction systems with similar geometries. Because phase shifting technology is typically only used on critical design levels (reduction reticles), the concern for transparent and transmission defects that could impact phase are not as significant for 1X reticles [9].

Many experiments and simulation studies have been undertaken to establish a threshold where these reticle defects impact yield by printing on wafers. However, none of these studies have actually examined the capability of inspection systems to capture and correctly categorize sub-half-micron defects on the reticle. It is important to correlate the defects as measured on the inspection system with the printing defects, in order to enhance reticle yields and control reticle manufacturing costs.

An additional consideration is that experimental and simulation studies are typically performed at nominal exposure and focus conditions for the lithography process and toolset. This condition is considered optimal because it represents the middle of a typical production process window. However, it has been recently recognized that it is important to study defect printability over the entire lithography process window [2, 10]. This is accomplished by simultaneously determining the focus and exposure latitudes that control CD variation within ± 10 percent of nominal.

This study furthers the understanding of the behavior of subhalf-micron defect types in 1X projection systems by evaluating defect detectability and defect printability over the lithography process window. The knowledge gained can then be extrapolated into reticle quality specifications that meet users' requirements and manufacturers' current and future capabilities.

2.0 EXPERIMENTAL METHODS

2.1 Reticle Design

The reticle design for this experiment was based on a metal layer for a 4 Mb DRAM shrunk down to a 0.65 μm design rule, which represents a 64 Mb process. This production mask design allowed for an unbiased examination of both mask manufacturing and inspection capabilities, as well as defect printability within standard production feature sizes. The die was repeated in a 9 x 7 array separated by 1.0 mm chrome spaces to cover a 44 x 22 mm field. A second field was written using the same die shrunk to a 1.0 μm design rule for an additional study using a different lithography system.

Two sets of defects were added to the metal layer. The following opaque and clear defect sizes (at CAD) were attached to 1.5 μm chrome lines in a large clear area: 0.15, 0.20, 0.25, 0.30, 0.40, and 0.50 μm . The effects of defects on line-width could thus be studied without the problems of small defect bridging in dense areas (see Figure 1a). To study the proximity effects of defects near line edges, duplications of the opaque defects were also placed in varying distances from the edges by 0.10 to 0.50 μm , in 0.10 μm increments (see Figure 1a). Clear holes were placed at the same sizes and distances from the edge of a large chrome feature (see Figure 1b). A third series of these opaque and clear defect sizes were placed in isolated locations (see Figures 1a and 1b). All of these defects were added as a separate pattern file to six of the dice within the field. A die-to-database inspection file was created with the defect file omitted.

The second set of defects was placed in a dense feature area which closely matched the design rule. CAD defect sizes of 0.20 x 0.20, 0.20 x 0.30, 0.30 x 0.30, 0.30 x 0.40, 0.40 x 0.40 and 0.40 x 0.50 μm were placed to create opaque and clear extensions, and isolated defects (see Figures 1c and 1d). Unlike the first set of defects, this second set was added to the metal pattern file and was therefore not inspectable on the reticle in either die-to-die or die-to-database mode.

The reticle was written on a MEBES 4500 using PBS resist. It was developed with a high resolution process, which is currently under engineering development at the photomask supplier. No data biasing was applied to the design data and CDs were held to within ± 0.03 μm of a nominal 0.65 μm chrome line. Reticle CDs were verified on a low voltage SEM.

Defect inspection was completed on an Orbot RT-8000 in a die-to-database mode. The database was fractured utilizing a special software feature requiring fracture of a single die only. This technique resulted in a fracture time under seven minutes and reduced disk space required to store the inspection file. The inspection stage speed was set for a 0.25 μm defect rate. A second auto-inspection was performed on a KLA 219HRS in die-to-die mode. The system was set up with a normal scan speed and an effective pixel size/minimum defect size of 0.25 μm .

2.2 Processing Conditions

Several 150 mm silicon wafers were used throughout this study. All wafers were vacuum-baked and HMDS primed prior to photoresist coating. JSR iX500EL photoresist manufactured by the Japanese Synthetic Rubber company was used throughout the investigation. A swing curve, generated in previous experiments, indicated an optimal photoresist thickness of 0.98 μm for 0.65 μm resolution. This location on the swing curve provides maximum process latitude. The photoresist was coated to the 0.98 μm target thickness using the process and equipment described in Table 1. Coating thickness and uniformity were verified on a Prometrix FT700 film measurement system. Photoresist thickness uniformity was held to $\pm 75\text{\AA}$ across each wafer. The postexposure bake and develop processes are shown in Table 2.

2.3 Lithography Equipment

All lithography was performed on an Ultratech Stepper Saturn Wafer Stepper® lithography system. The Ultratech stepper is based on the 1X Wynne-Dyson lens design employing broadband i-line illumination from 355 to 375 nm [11]. The Ultratech Saturn has a numerical aperture (NA) of 0.365 and is specified at 0.65 μm resolution, with 1.5 μm DOF, and a field size of 44 x 22 mm. To obtain the maximum information from each wafer, 15 fields with unique conditions were exposed on each wafer. The layout consisted of a three by five array as illustrated in Figure 2. Exposure was varied from 155 to 215 mJ/cm^2 , and focus was varied from -2 to +2 μm , to determine the process window. The nominal exposure conditions were determined by exposing a wafer and measuring the desired CD on a Hitachi S-7280 SEM. Nominal exposure dose was determined to be 170 mJ/cm^2 with an optimal defocus setting of 0 μm .

3.0 RESULTS AND DISCUSSIONS

3.1 Reticle Inspection

A total of 864 defects were added to the 0.65 μm design rule field. Half of these were less than 0.30 μm CAD size and were not expected to resolve. This was especially true for the isolated pinholes and chrome spots as well as the proximity defects separated by $>0.20\ \mu\text{m}$. An optical microscope inspection of the reticle indicated that the pinholes placed at 0.10 μm separation from a feature corner resulted in corner rounding at 0.25 μm (CAD) and larger. Pinholes placed at $>0.10\ \mu\text{m}$ from line and corner edges barely resolved at the 0.40 μm (CAD) size.

Inspection system “A” found a total of 205 defect areas and system “B” found 155 total for the six die containing programmed defects. Because most of the programmed defects of a given size were placed too close together, the machines only counted the first defect encountered in the inspection window. A total of 64 percent of the defects in the 0.65 field were measured at $\leq 0.50\ \mu\text{m}$.

The defect capture analysis is taken from a single die sample to minimize any potential damage from the SEM measurement technique. Optical microscope inspection indicated that most of the defects that were measurable in that particular die also appeared to be resolved in the other five die with programmed defects. Defect map coordinates for the reticle autoinspection equipment also indicated that the same defects were captured in each die with programmed defects. SEM measurements of the defects correlated to the inspection equipment measurements within $\pm 0.05 \mu\text{m}$.

Half of the chrome defects measuring 0.10 to 0.15 μm on the reticle were captured by the inspection equipment (Figure 3a). When the defect size increased to 0.15 to 0.20 μm , the capture rate increased to 83 percent. All chrome defects $\geq 0.20 \mu\text{m}$ were captured within the inspection window.

There were two clear edge defects measuring 0.15 and 0.16 μm on the reticle. One of these was captured (Figure 3b). There were no defects of this type in the 0.20 to 0.25 μm range. There were two pinholes in the 0.30 to 0.35 μm range, and both eluded capture. Both were separated from the chrome feature edge by at least 0.20 μm . All pinhole and clear edge defects $>0.35 \mu\text{m}$ were captured.

3.2 CAD to Reticle Resolution

SEM inspection and measurement revealed a high degree of defect resolution on the reticle. After confirmation of the nominal 0.65 μm chrome line CD value, each of the programmed defects was measured. In the large feature area, opaque defects as small as 0.15 μm (CAD) had resolved sufficiently to effect linewidth by 0.11 μm (Figure 4a). At 0.10 μm separation from line edge, the defects partially resolved and bridged to the lines, creating slightly larger linewidth increases than the same size defects (at CAD) attached to the edges (0.17 versus 0.11 μm). At defect sizes of 0.15 to 0.40 μm (CAD), as the defect to line edge designed distance increased to 0.20 and 0.30 μm , the bridging disappeared and the linewidth variation decreased relative to the 0.10 μm separation. For example, the 0.50 μm (CAD) defect size increased to 0.57 and 0.65 μm at 0.10 and 0.20 μm separations and then decreased to 0.41 μm at both 0.30 and 0.40 μm separation.

Defects placed in proximity to feature intersections had an obvious visual effect on corner resolution. For opaque defects, this effect began at 0.15 μm separated by 0.10 μm , and clear defects became visible at 0.25 with a 0.10 μm separation. The resulting rounded geometry corners were not measurable with the available SEM configuration.

The clear defects in the large feature area behaved somewhat differently from the opaques. The first measurable linewidth variation (-0.15 μm) was at the 0.20 μm (CAD) defect attached to the chrome line edge. At a 0.10 μm and greater separation from line edge, the clear defects (pinholes) designed at $\leq 0.30 \mu\text{m}$ were unresolved and did not effect reticle linewidth. The 0.40 and 0.50 μm designed defects at 0.10 μm separation measured 0.39 and 0.49 μm , respectively, on the reticle (Figure 4b). Each of these pinholes reduced in size as the separation from line edge increased,

until finally disappearing at 0.40 μm distance. All of the clear defects attached to the chrome line edges measured about 0.10 μm smaller than their designed size.

In the dense feature area, the programmed defects were susceptible to grid snapping during E-beam write, which has contributed to reticle defect sizes being somewhat larger than designed. However, they provide valuable information regarding reticle-to-wafer defect impact in this design rule. All of the clear defects attached to a line edge, from 0.26 x 0.23 μm to 0.62 x 0.50 μm , appeared on the reticle. Isolated clear pinholes began to appear at 0.33 x 0.32 μm . Opaque edge defects were measurable up to 0.45 X 0.40 μm at which point bridging occurred in the 0.60 μm space. Isolated opaque defects (in the same space) appeared at 0.18 μm and began bridging at 0.49 μm .

3.3 Wafer Exposure Process Window Determination

A series of focus exposure matrices was processed on each wafer, and then CDs were measured on the SEM to determine the nominal focus and exposure settings for the stepper and lithographic process. A Bossung plot of CDs through these various stepper settings was used to indicate the minimum and maximum settings for a ± 10 percent process window (Figure 5). Nominal exposure/focus was 170 mJ/cm^2 at 0 μm defocus. The minimum settings were 155 mJ/cm^2 at both -1.0 and +1.0 μm defocus. The maximum exposure energies and focus settings for the process window were determined to be 200 mJ/cm^2 at -1.0 μm and 185 mJ/cm^2 at +1.0 μm defocus. Both opaque and clear defects were measured at the nominal focus and exposure dose as well as the four corners of the process window. Figures 6a through 6e indicate that the differences in opaque defect sizes for the same reticle defect at the various wafer exposure fields were in the 20 to 40 nm range. It is apparent that similar contours are observed for all of the plots in Figure 6, indicating that defect printability is consistent throughout the process window. Some of the plot contours are irregularly shaped because there were numerous data points reflecting 0 defect separation from line edge and a relative few points where defects were both separated on the reticle and resolved on the wafer.

3.4 Reticle-to-Wafer Resolution

3.4.1 Large Area Chromes

Defects of all types at 0.15 μm (CAD) had no discernible effect on the wafer.

The first reticle defect that had a notable effect on the wafer was a 0.21 μm chrome extension. At the nominal exposure field, this defect resulted in a 0.07 μm linewidth delta on the wafer. However, at the remaining exposure fields, the average linewidth change was only 0.028 μm (Figures 6a through 6e). Another chrome extension defect at 0.26 μm resulted in a 0.07 μm linewidth change on the wafer at the nominal field, but only a 0.058 μm average change across the process window (Figures 7b and 7c). A third 0.25 μm chrome extension changed the line CD by 0.09 μm at nominal and 0.08 μm average. Allowing for a ± 0.01 μm measurement error, it appears

that 0.20 μm chrome extensions on a reticle will not violate a ± 10 percent CD rule for a 0.65 μm device. Chrome extensions at 0.25 μm , however, are likely to produce marginal results on 0.65 μm wafers. Fortunately, this size and type of defect was easily identified on the test reticle with current inspection equipment.

On the other hand, isolated chrome spots measuring 0.27 μm on the reticle had no measurable effect on the wafer (Figures 7d and 7e). A chrome spot that is both 0.33 μm in size and within a 0.20 μm proximity to a line edge, increased the line by 0.12 μm average. When the same size defect was 0.33 μm away from the line, it only changed the CD by 0.07 at the nominal field and only 0.054 μm average. The 0.41 μm spot behaved similarly at 0.29 and 0.44 μm separations. With one or two possible exceptions, all of the 0.30 through 0.50 μm chrome spots within 0.20 to 0.30 μm of a line create trouble for the 0.65 μm device. Again, reticle defects at that size are easily detectable. Chrome spots as large as 0.40 μm did not print on the wafer when isolated by a sea of glass. They are too small to resolve with the stepper NA at 0.365.

3.4.2 Large Area Clear Defects

The 0.20 μm (CAD) clear edge defect translated to a -0.15 μm clear extension on the reticle (Figure 7a). On the wafer, this resulted in small linewidth reductions of 0.07 μm at the nominal field, but averaging 0.054 μm across the five fields of the process window. A second clear extension measuring 0.16 μm on the reticle translated to 0.06 μm at the nominal wafer field and averaged 0.054 μm across the window.

The first clear defect to notably affect the wafer was an extension measuring 0.29 μm on the reticle. This defect reduced the opaque linewidth by an average 0.2 μm (Figures 7d, 7e, and 8). In another area of the reticle pattern, both a 0.39 and a 0.49 μm clear hole placed at 0.1 μm proximity to a clear line increased the clear linewidth on the wafer by an average 0.19 μm (Figures 1b 9a through 9d). However, when placed at 0.20 μm separation from the line edge, one of the pinholes, despite measuring 0.31 μm on the reticle, was unresolved on the wafer. A 0.41 μm pinhole placed at the 0.20 μm separation increased the clear linewidth by 0.12 μm (Figures 9e and 9f). The largest pinhole at 0.30 μm separation measured 0.34 μm and failed to resolve on the wafer. A 0.34 μm pinhole does not allow enough light through to expose resist.

In the 0.65 μm design rule area, opaque lines measured 0.82 μm and clear spaces measured 0.59 μm on the wafer. A chrome extension measuring 0.23 x 0.19 μm on the reticle changed linewidth by only 0.06 μm (Figures 1d, 10a, and 10b). An isolated chrome spot at 0.18 μm on the reticle caused a 0.05 μm change. All other chrome extensions and spots larger than 0.30 μm violated the ± 10 CD rule, usually by bridging.

Again in the 0.65 μm design rule area, clear extensions on the reticle yielded mixed results. One extension measuring 0.34 x 0.23 μm changed the opaque linewidth by only 0.06 μm . A second extension at 0.26 x 0.23 μm created a 0.07 μm wafer linewidth change (Figures 1c, 10c, and 10d). All of the 0.37 μm and larger extensions changed linewidth by a minimum 0.15 μm . The smallest

isolated clear pinhole to resolve on the reticle measured $0.33 \times 0.32 \mu\text{m}$ and caused a linewidth change on the wafer of $0.11 \mu\text{m}$. A $0.44 \times 0.47 \mu\text{m}$ pinhole is illustrated in Figures 10e and 10f.

4.0 CONCLUSIONS

It has been demonstrated that clear and chrome reticle defects exhibit similar behavior with the 1X projection lithography systems and with 5X reduction systems [1, 12]. In both cases, printability is affected by defect proximity to a line as well as defect size. It was determined that changes in exposure and focus that held CDs to ± 10 percent had little effect on wafer defect size. However it was also indicated that defects that have marginal impact at a nominal focus/exposure setting could be rendered ineffective by slight adjustments within that window.

Autoinspection of the reticle produced mixed results. Because many of the programmed defects were positioned too closely together, inspection results were difficult to quantify. However, it was demonstrated that chrome defects at $0.20 \mu\text{m}$ and larger were consistently captured in each die containing defects on the test reticle. This is good news because it has also been demonstrated that an opaque reticle defect as small as $0.20 \mu\text{m}$ has the potential to violate the commonly used 10 percent CD rule for a $0.65 \mu\text{m}$ device in 1X lithography.

While some clear defects at $<0.30 \mu\text{m}$ were captured, other larger ones were missed. Because only one inspection run was performed on each piece of production equipment, it is possible that better results could be obtained with additional inspection in an optimized environment. However, it is also important to note that all of the clear defects, from $0.16 \mu\text{m}$ and larger, that were either attached to a line edge or close enough to it to affect the wafer, were captured by the inspection equipment. Only those pinholes that were removed from a line edge by $0.20 \mu\text{m}$ or more were not detected, and they did not create any linewidth reductions or defects on the wafer. Because it has been determined that clear extension type defects at $0.25 \mu\text{m}$ are at the margin of adversely impacting linewidth in a $0.65 \mu\text{m}$ design rule, it is important to continue the investigation of clear defect detectability within a pattern designed to those rules.

5.0 ACKNOWLEDGEMENTS

The authors would like to thank a number of people for their assistance and contributions to this project. Calvin Ho in the Ultratech Stepper Reticle Engineering Department for providing assistance with the reticle design, reticle layout, and SEM measurements. James Justen in Ultratech Stepper's product marketing department gave advice and assistance in obtaining vendor participation. Alan Walther in Ultratech Stepper's Reticle Engineering department assisted with the reticle design.

We would also like to thank Ofer Hebron, Orbot customer support coordinator, for assistance with the reticle inspection and defect review. Jim Campi, Photronics special support manager, supported reticle manufacture and inspection. Terri Lampe, Photronics technical support analyst, ensured timely movement of the reticle through manufacture and inspection. Toby Panattoni, Photronics engineering group leader, provided reticle inspection and contributions to this paper on the Orbot inspection equipment and reticle manufacturing.

Finally, we would like to thank K.C. Wang of the Hewlett-Packard Marketing staff for assistance with the reticle inspection.

6.0 REFERENCES

1. B. J. Grenon, K. D. Badger, M. J. Trybendis, "Reticle Defect Sizing and Printability," *Symposium on Photomask Technology and Management Proceedings*, SPIE **1604** (1991).
2. P. Yan, J. Langston, J. Neff, R. Chatterjee, "Mask Defect Printability and Wafer Process Critical Dimension Control at 0.25 μm Design Rules," *Bacus News*, **12** (1) Jan 1996.
3. T. Kikuchi et.al., "Effects of Subhalf-Micron Defects on Wafer Images During VLSI Circuit Production," *Optical/Laser Microlithography II Proceedings*, SPIE **1088** (1989).
4. J. N. Wiley, J. A. Reynolds, "Device Yield and Reliability by Specification of Mask Defects," *Solid State Technology*, **36**(7), July 1993.
5. M. Rieger, J. Stirniman, "Customizing Proximity Correction for Process-Specific Objectives," *Optical Microlithography IX Proceedings*, SPIE **2726** (1996).
6. J. Sohn, S. Choi, B. Kim, H. Cho and H. Yoon, "Mask Technology for 0.18 Micron Device Generation," *Bacus News*, **12**(7) July 1996.
7. C. P. O'Mahony and K. Zollinger, "Defect Printability and 1X Reticles," *BACUS Fifth Annual Symposium Proceedings* (1985).
8. G. Flores, W. Flack and J. Cossins, "The Implementation and Characterization of Advanced Mix-and-Match Lithography," *Environmental Productivity and Defect Issues in Semiconductor Manufacturing Proceedings*, SEMICON/Europa Technical Conference (1994).
9. L. Zurbrick, S. Schuda, J. Wiley, "Effects of Transparent and Transmission Reduction Reticle Defects," *Optical/Laser Microlithography VIII Proceedings*, SPIE **2440** (1995).
10. L. Karklin, "A Comprehensive Simulation Study of the Photomask Defects Printability," *Symposium on Photomask Technology and Management Proceedings*, SPIE **2621** (1995).
11. R. Hershel, "Characterization of the Ultratech Wafer Stepper," *Optical Microlithography Proceedings*, SPIE **334** (1982).

12. J.N. Wiley, "Process Effect in 5X Reticle Defect Printability", *Symposium on Photomask Technology and Management Proceedings*, SPIE **1064** (1989).

Process Step	Parameters	Equipment
Vacuum Bake, HMDS vapor-prime		YES LP-3 Oven
Manual photoresist dispense	10ml JSR Resist, static dispense	Solitec 5110C
Spread	2 seconds at 1000 RPM	Solitec 5110C
Spin	30 seconds at 2950 RPM	Solitec 5110C
Softbake	60 seconds at 100°C	MTI Flexifab system

Table 1: Photoresist process and equipment

Process Step	Parameters	Equipment
Postexposure bake	60 seconds at 120°C	MTI Flexifab track system
Batch develop	60 seconds, PD 523 developer at 25°C	Wafer processing systems wet-sink
Rinse/spin-dry		Semitool

Table 2: Postexposure bake and develop processes

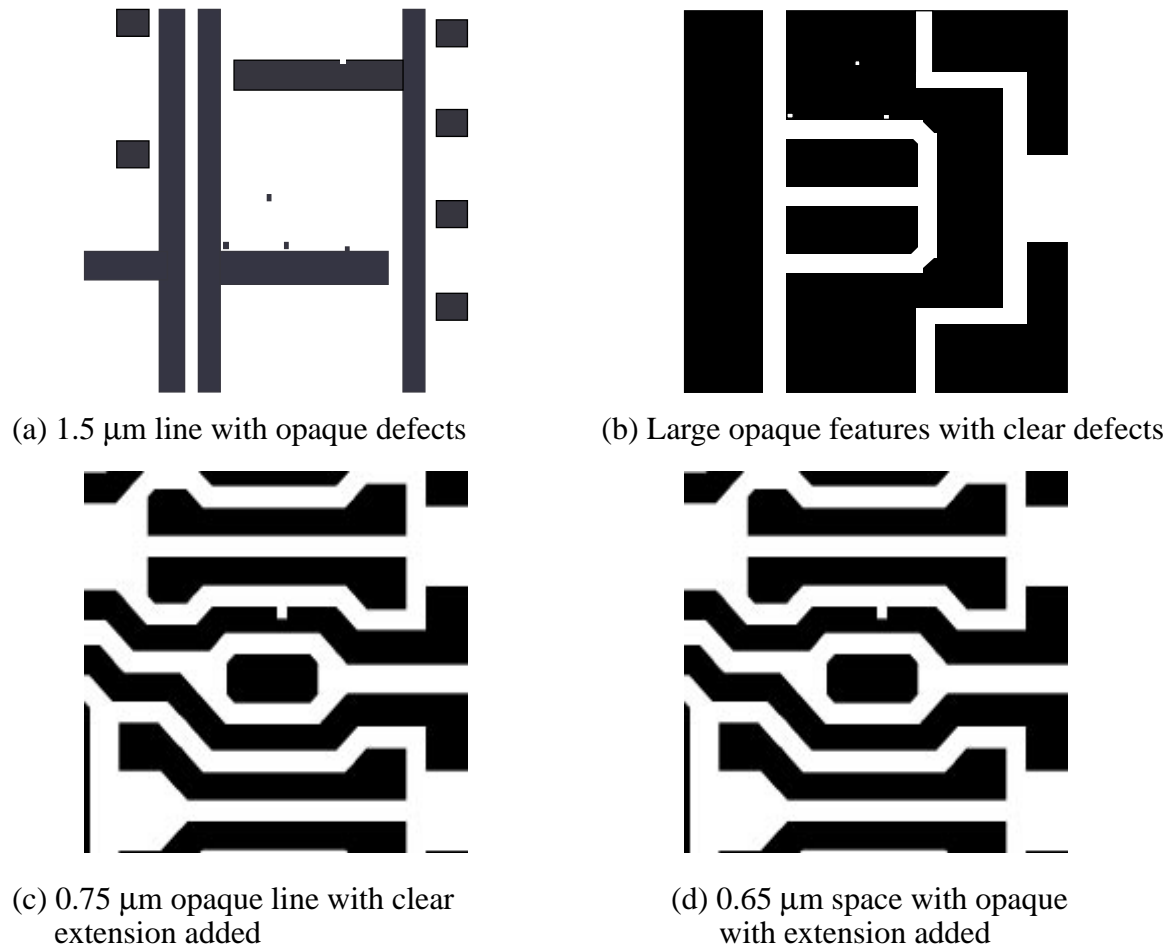


Figure 1: Reticle CAD drawings showing the opaque and clear pinhole defects added to the DRAM design

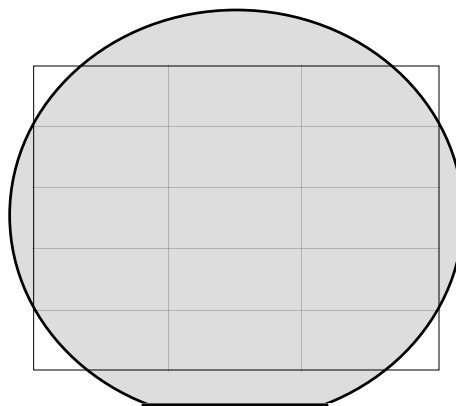
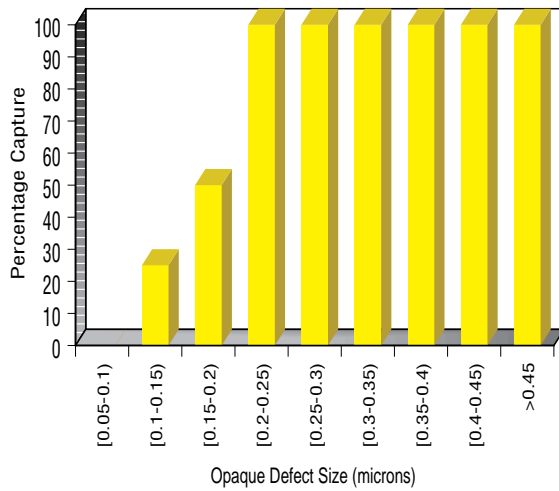
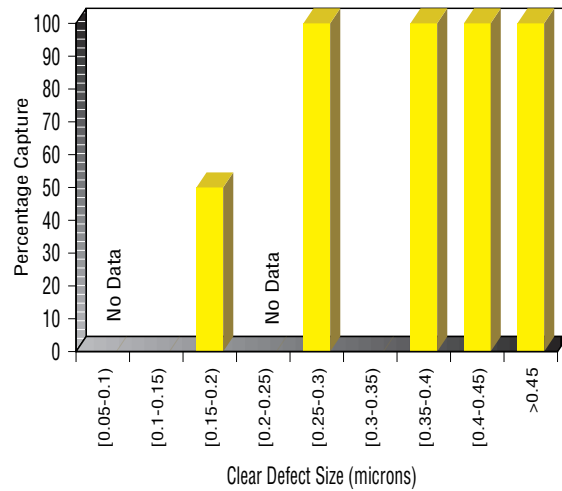


Figure 2: Wafer map showing 15 field focus and exposure matrix

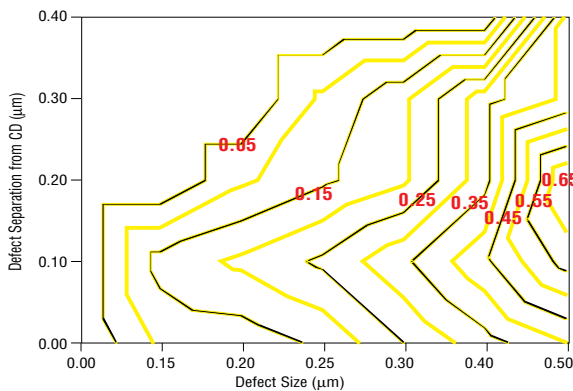


(a) Opaque Defects Captured

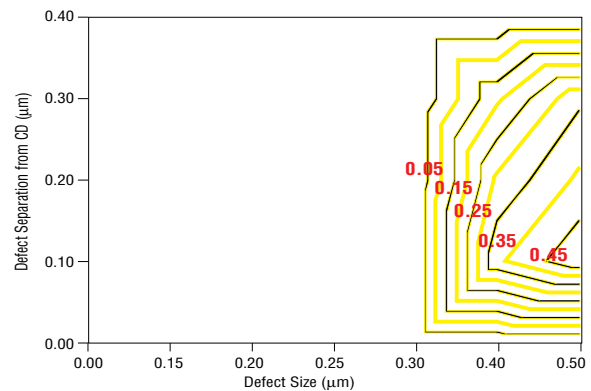


(b) Clear Defects Captured

Figure 3: Reticle defect capture at autoinspection. The defect size is as measured on the reticle



(a) CAD to reticle opaque defect resolution



(b) CAD to reticle clear defect resolution

Figure 4: CAD to reticle defect resolution for opaque and clear defects. The separation and defect size are as drawn (CAD). The contours represent the size on the reticle in microns

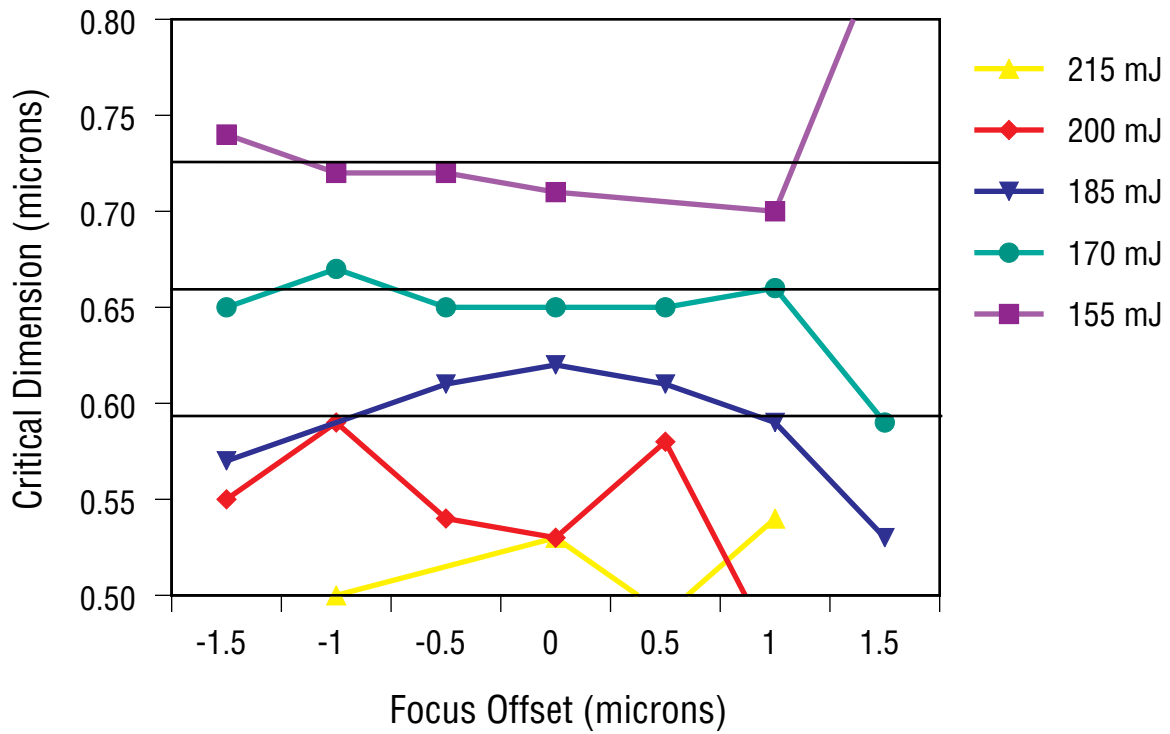
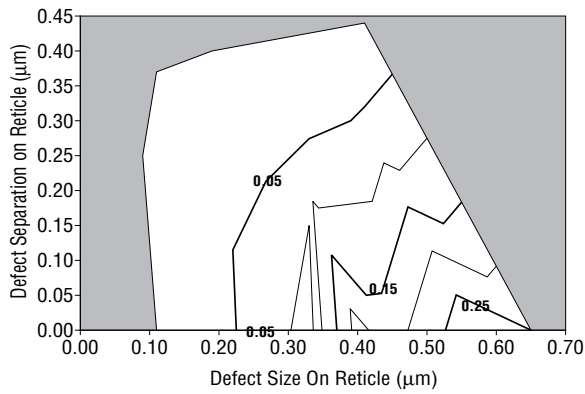
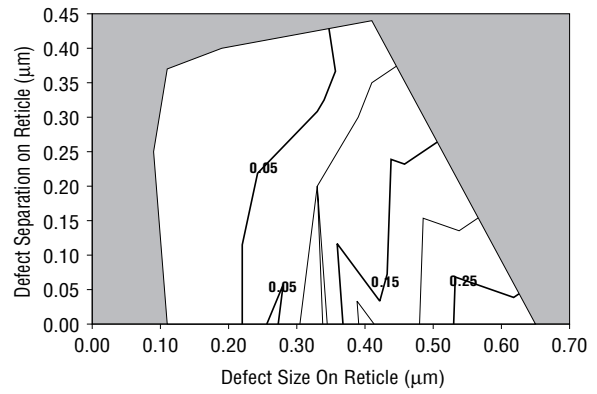


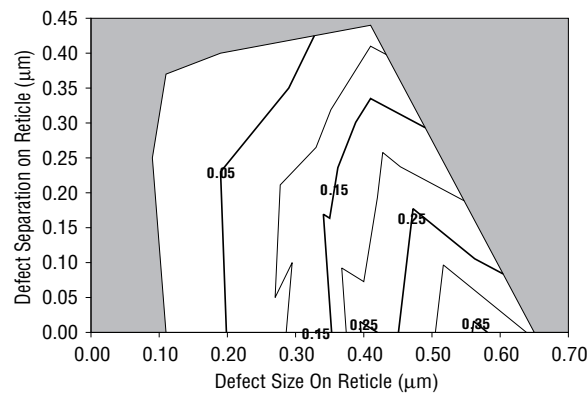
Figure 5: Bossung plot for JSR 500 photoresist on an Ultratech Saturn Stepper. The nominal line size is 0.65 μm with ± 10 percent control limits



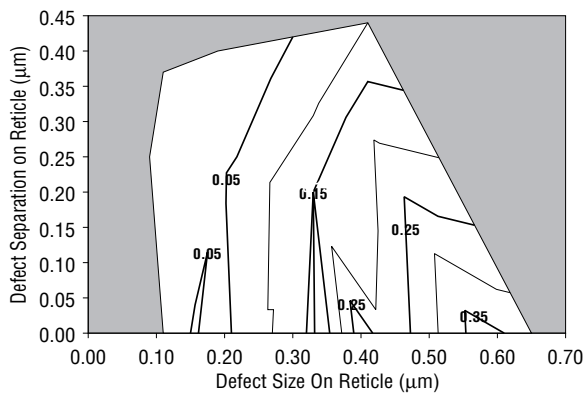
(c) Focus = -1 μm , Exposure = 200 mJ/cm^2



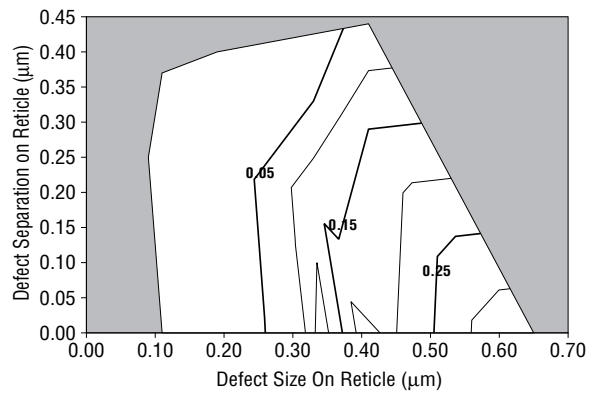
(e) Focus = 1 μm , Exposure = 185 mJ/cm^2



(a) Focus = 0 μm , Exposure = 170 mJ/cm^2

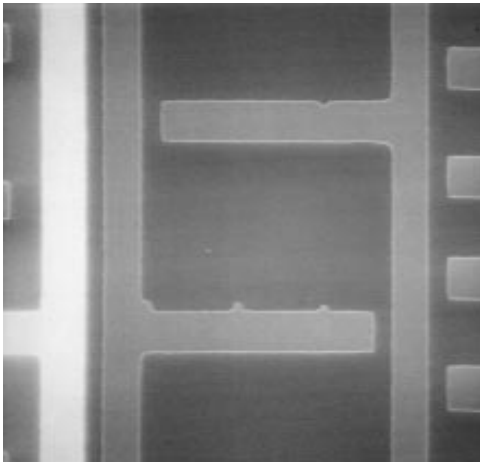


(b) Focus = -1 μm , Exposure = 155 mJ/cm^2

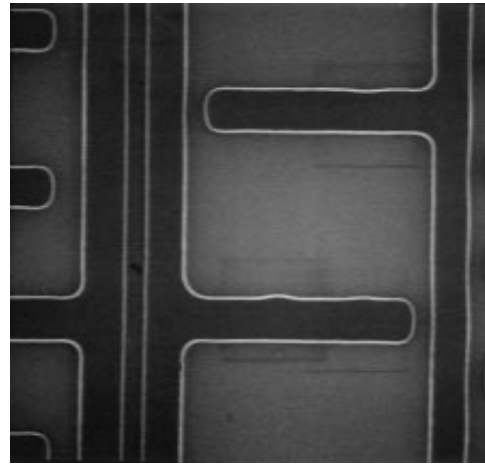


(d) Focus = 1 μm , Exposure = 155 mJ/cm^2

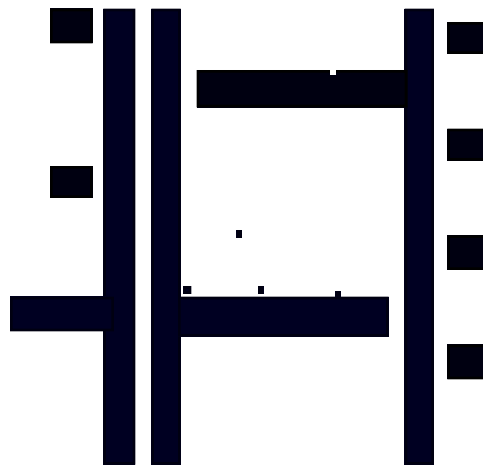
Figure 6: Reticle to wafer opaque defect resolution across the lithography process window. The separation and defect size are as measured on the reticle. The contours represent the size on the wafer in microns



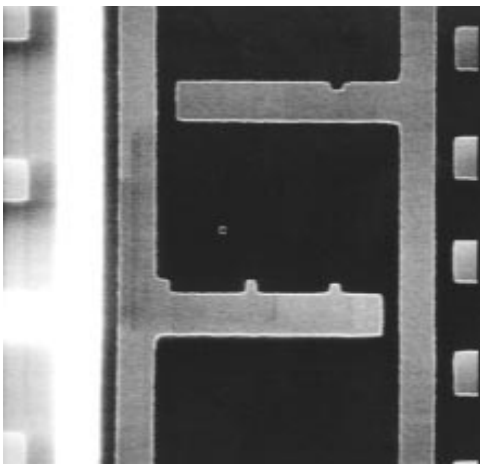
(b) 0.26 μm chrome extension on reticle



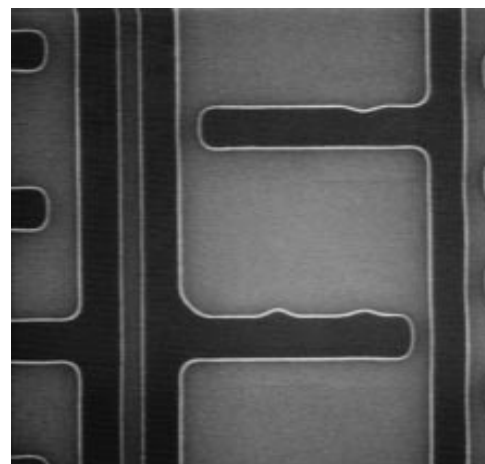
(c) 0.058 μm opaque extension on wafer



(a) CAD plot of opaque defect area



(d) 0.29 μm clear extension on reticle



(e) 0.20 μm clear extension on wafer

Figure 7: Comparison of extensions on the reticle and wafer at 20k magnification

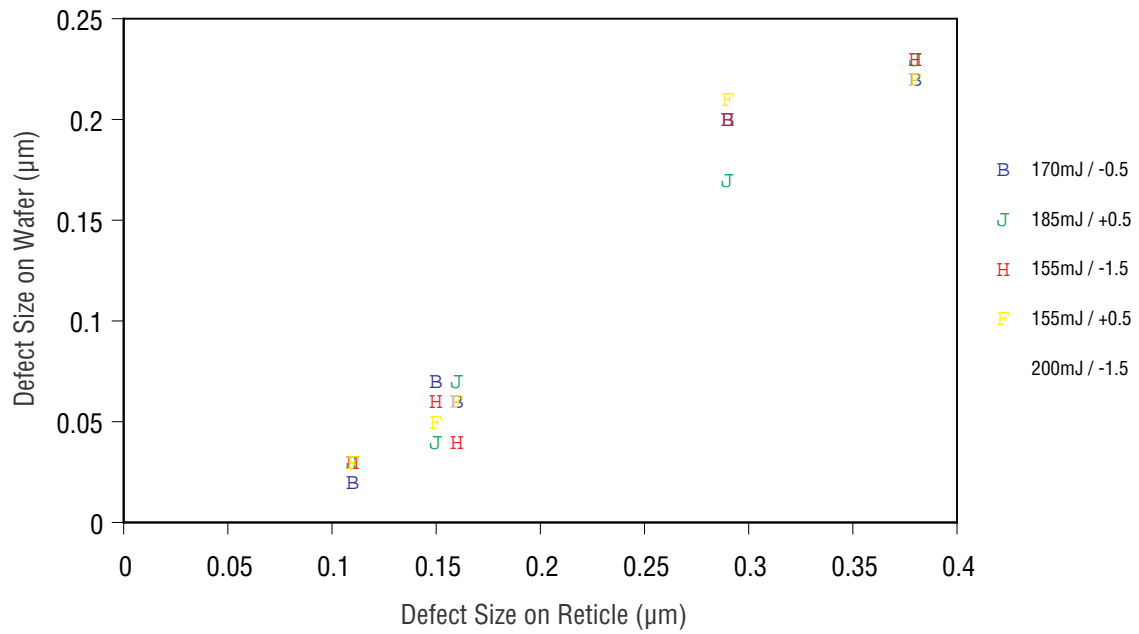
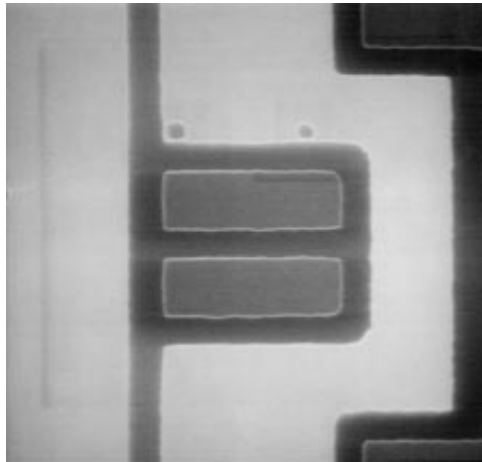
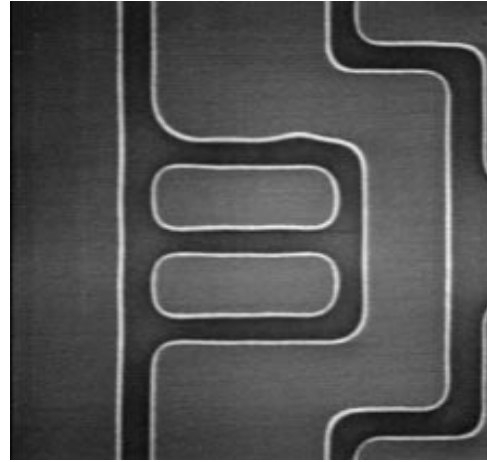


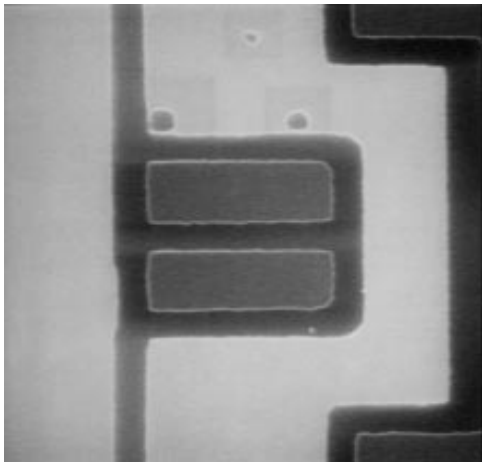
Figure 8: Reticle to wafer clear edge defect resolution. The defect size is as measured on the reticle



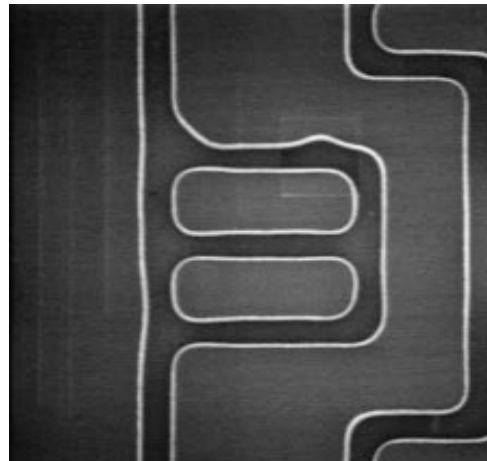
(a) 0.39 μm clear hole on reticle



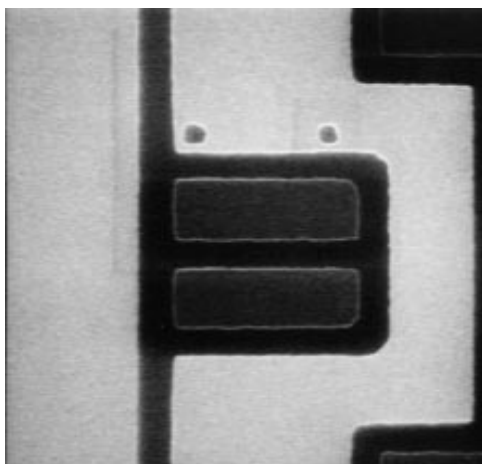
(b) 0.194 μm clear extension on wafer



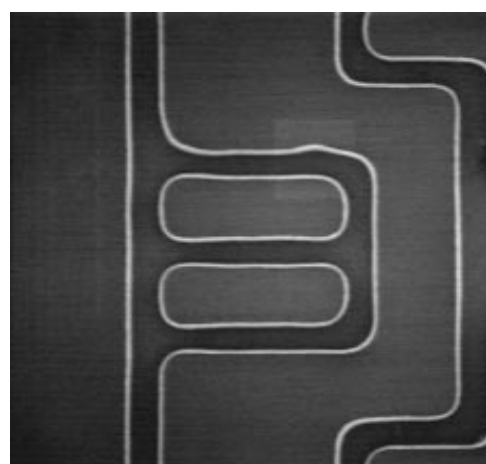
(c) 0.49 μm clear hole on reticle



(d) 0.19 μm clear extension on wafer

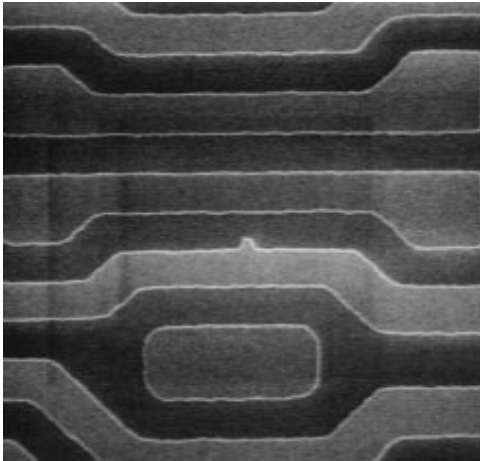


(e) 0.41 μm clear hole on reticle



(f) 0.12 μm clear extension on wafer

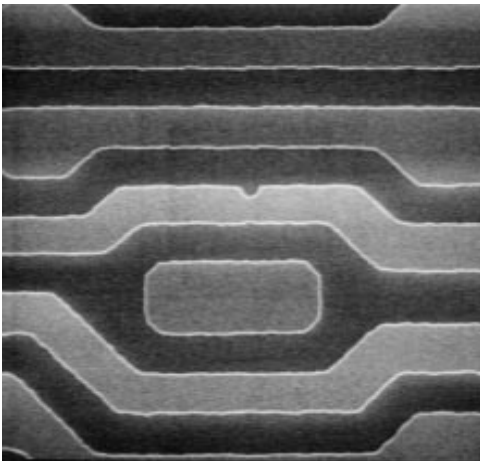
Figure 9: Comparison of a clear hole on the reticle and wafer at 20k magnification



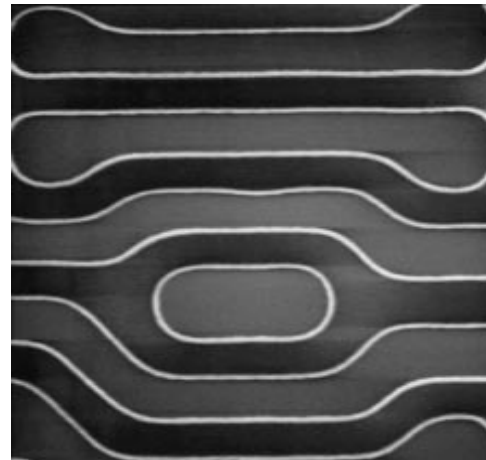
(a) $0.23 \times 0.19 \mu\text{m}$ chrome extension on reticle



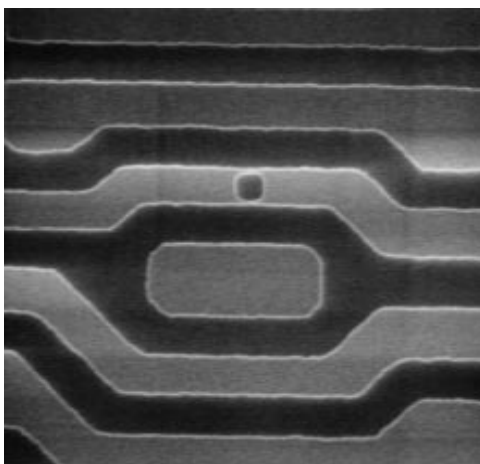
(b) $0.06 \mu\text{m}$ opaque extension on wafer



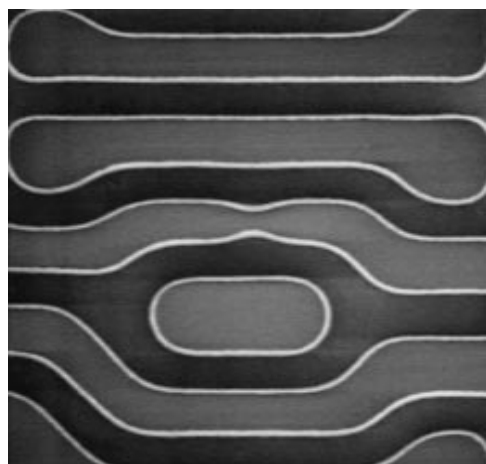
(c) $0.26 \times 0.23 \mu\text{m}$ clear extension on reticle



(d) $0.07 \mu\text{m}$ clear extension on wafer



(e) $0.44 \times 0.47 \mu\text{m}$ isolated clear on reticle



(f) $0.31 \mu\text{m}$ isolated clear on wafer

Figure 10: Comparison of extensions and holes on the reticle and wafer at 20k magnification